Special Issue of the Bulletin of the Iranian Mathematical Society
Vol. 37 No. 2 Part 1 (2011), pp 117-131.

PAIRED ANISOTROPIC DISTRIBUTION FOR IMAGE SELECTIVE SMOOTHING

A. MADANKAN

Communicated by Ale Jan Hombürg

Abstract. In this paper, we present a novel approach for image selective smoothing by the evolution of two paired nonlinear partial differential equations. The distribution coefficient in de-noising equation controls the speed of distribution, and is determined by the edge-strength function. In the previous works, the edge-strength function depends on isotropic smoothing of the image, which results in failing to preserve corners and junctions, and may also result in failing to resolve small features that are closely grouped together. The proposed approach obtains the edge-strength function by solving a nonlinear distribution equation governed by the norm of the image gradient. This edge-strength function is then introduced into a well-studied anisotropic distribution model to yield a regularized distribution coefficient for image smoothing. An explicit numerical scheme is employed to efficiently solve these two paired equations. Compared with the existing methods, the proposed approach has the advantages of more detailed preservation and implementational simplicity. Experimental results on the synthesis and real images confirm the validity of the proposed approach.

MSC(2000): Primary: 35M13; Secondary: 65D19.
Keywords: Computer vision, anisotropic distribution, Image smoothing, partial differential equation.
Received: 21 August 2008, Accepted: 27 June 2009.

1. **Introduction and preliminaries**

One major task in computer vision and image processing is to smooth images that are corrupted by noise from the physical world and the imaging apparatus. Many different techniques are developed to deal with this challenging problem in the recent past, so it is infeasible to review all of them in this paper. Instead, we will briefly discuss a more promising and interesting technique that is the anisotropic distribution approach with the elegant formulation firstly introduced by Perona and Malik [15]. The underlying principle behind anisotropic distribution is that a family of increasingly smoothed images $u(x, y, t)$, defined in a domain $\Omega \subset \mathfrak{R} \times \mathfrak{R}$, can be obtained as the intermediate states of a distribution equation with the original image $u(x, y, 0)$ as the initial state. This approach gave impressive results, and overcame the linear filters drawbacks [24] including blurred edges, hights of the locations of features at the coarse from their true locations and destruction of edge junctions are destroyed. Since then, numerous researchers have been devoted themselves to theoretical and practical understanding of this and related methods for image smoothing and edge detection, such as regularizing anisotropic distribution [2, 21], modifying for range image [12, 19], defining the well-posed conditions [26], determining the optimal stopping time for anisotropic distribution [7, 11] and studying the relationship between the anisotropic distribution and other image processings [3, 16]. Comprehensive reviews of anisotropic distribution can be found in [17, 23]. Some distribution equations related to our work will be further explained in Section 2. Numerical results indicate that the choice of v, which is an edge strength function, plays a very important role in the quality of the recovered images.

Here, we will present a regularized distribution coefficient which depends on a novel function v. After that, we obtain an anisotropic distribution model constituted of two paired partial differential equations, and use a concise and efficient explicit scheme to solve them. The proposed distribution coefficient not only contributes to the removal of noise from original images, but also preserves the detail features well. The remainder of our work is organized as follows. In Section 2, some anisotropic distribution algorithms are outlined. In Section 3, the function v is achieved by solving a nonlinear distribution equation which depends on the norm of the image gradient. Then, the anisotropic smoothed version

of norm, the function v, is introduced into a well-studied image smoothing anisotropic distribution equation to form a regularized distribution coefficient. The explicit numerical schemes can be used to efficiently solve these two equations. In Section 4, experimental results on the synthesis and real images are presented, and performance comparisons between the proposed algorithm and the one due to Catte et al. [4] are given. Conclusions are given in Section 5.

2. **Outline of anisotropic distribution**

distribution algorithms remove noise from an image by modifying the image via a partial differential equation. One property of anisotropic distribution is to integrate prior knowledge of the image into the distribution coefficient. Perona and Malik [15] first introduced the idea of nonlinear distribution that is preferred within a smooth region to distribute near an edge. They proposed the enhancement of image I by the solution of the following partial differential equations:

$$\begin{cases} \frac{\partial u}{\partial t} = div[g(|\nabla u|)\nabla u], \\ u(x,y,0) = I(x,y) \\ \frac{\partial u}{\partial t}|_{\nabla\Omega} = 0, \end{cases} \tag{2.1}$$

where, ∇u denotes the local image gradient, $\partial\Omega$ denotes the boundary of Ω, n represents the direction normal to $\partial\Omega$, and the distribution coefficient $g(.)$ is a non-negative function of the magnitude of local image gradient. It has such properties as: $g(0) = 1, g(s) \geq 0$ and $g(s) \to 0$ as $s \to \infty$. If g is constant, the model of anisotropic distribut in (2.1) reduces to the classical Gaussian filtering, whereas in the Perona and Maliks model, two usual choices for $g(.)$ are suggested

$$g_1(s) = exp\left[-\left(\frac{s}{k}\right)^2\right] \ and \ g_2(s) = exp\left[1 + \left(\frac{s}{k}\right)^2\right]^{-1} \tag{2.2}$$

where, k is a constant and should be tuned for a specific application. Since the two proposed distribution coefficients make the distribute process perform selective smoothing, which depends on the magnitude of image gradient at the point, the edges remain sharp and undistorted across many scales. Thus, it yields stable edges across many scales. So, it is not necessary to track edges across the scale space, which is a complicated and expensive task. However, the anisotropic distribution process introduced by Perona and Malik does not perform well for large

noisy images, and very similar images could produce divergent solutions, as pointed out in [4]. The problem is mainly due to the dependence of the variable distribute coefficient $g(|\nabla u|)$ on the magnitude of the image gradient. If the initial image I is very noisy, then large oscillations in $|\nabla I|$ and hence in $|\nabla u|$ will result in a large number of false edges. To alleviate this problem, Catte et al. [4] introduced a Gaussian smoothing operation to the variable s of the distribution coefficient $g(s)$. Their model is formulated as follows:

$$\frac{\partial u}{\partial t} = div[g(|\nabla(G_\delta * u)|)\nabla u], \tag{2.3}$$

where, $G_\delta * u$ denotes a convolution of the image at time t with a Gaussian kernel. Although this change results in much improvement in the smoothing procedure, Gaussian convolution is an isotropic distribution. This leads not to preserve some important features well. In addition, a question that needs to be answered before applying the distribution process is what size Gaussian kernel should be used to smooth the image.

Note that although the distribution coefficient in (2.1) is a scalar, Perona and Malik [15] implemented the anisotropic distribution process by making the the distribution coefficient in each of the four diffusing directions depend on the directional gradient in that direction. Alvarez et al. [1] further extended their work by modifying the distribution operator,

$$\frac{\partial u}{\partial t} = g(|\nabla(G_\delta * u)|)|\nabla u| div\left(\frac{\nabla u}{|\nabla u|}\right). \tag{2.4}$$

This process is anisotropic and has a geometric interpretation, it diffuses u in the direction orthogonal to its gradient ∇u and does not diffuse at all in the direction of the gradient ∇u.

Image smoothing can also be achieved by variational methods [5, 8, 21, 10, 14, 20] through modifying or regularizing the anisotropic distribution. Here, we will only emphasize two more for the purpose of motivation. Mumford and Shah [13] proposed an algorithm to perform simultaneous image de-noising and segmentation by minimizing the following functional,

$$E(u, B) = \int_{\Omega/B} |\nabla u|^2 dx + \int_\Omega \beta|u - I|^2 dx + |B|, \tag{2.5}$$

where, the smoothed image u is assumed to be piece-wise constant, and B represents the edges of the true image. Since it is difficult to apply gradient descent method with respect to B, Shah [18], by introducing an

edge-strength function v, which takes values close to one on the edges, and rapidly decays away from the edges to value zero in homogeneous regions, proposed the model for image de-noising and segmentation as follows:

$$E_s(u,v) = \int_\Omega \left\{ \alpha(1-v)|\nabla u|^2 + |u-I| + \frac{\rho}{2}|\nabla v|^2 + \frac{v^2}{2\rho} \right\} dx. \tag{2.6}$$

The Euler-Lagrange equation on (2) is computed, and can be solved by using a dynamic scheme:

$$\begin{cases} \dfrac{\partial u}{\partial t} = -2\nabla v.\nabla u + (1-v)||\nabla u||div(u) - \dfrac{\beta}{\alpha(1-v)}||\nabla u||\dfrac{u-I}{|u-I|} \\ \dfrac{\partial v}{\partial t} = \nabla^2 v - \dfrac{v}{\rho^2} + \dfrac{2\alpha}{\rho}||\nabla u||. \end{cases} \tag{2.7}$$

Replacing the length functional in E by the last two terms in E_s renders the method more amenable to solving by means of the evolution equations. In addition, we observe that the first term in Es is of the TV type that reduces the amount of smoothing across edges. However, even with this modification, Shah's algorithm still results in an isotropic smoothing of v and rounded edges at times.

Here, a novel paired nonlinear partial differential equation model is proposed on the basis of the analysis of previously mentioned models. The goal is to obtain a method for image enhancement which has the capability of preserving edge features in large noisy images.

3. **Paired anisotropic distribution**

3.1. **Requirements on distribution coefficient.** Among the models mentioned in the last section, the choices of function v in the distribution coefficient include the equation $v = |\nabla u|$ in Perona and Malik's model,$v = |\nabla(G * u)|$ suggested by Catte et al., and the equation $\frac{\partial v}{\partial t} = \nabla^2 v - (v/\rho^2) + (2\alpha/\rho)(1-v)||\nabla u||$ mentioned in Shah's algorithm, and so on. Numerical simulations and experimental results show that the choice of the function v plays a very important role in the recovered quality of images contaminated by noise, so care must be taken in its determination. We note that all these function v in the distribution coefficients described in the previous section are isotropic, thus the distribution algorithm will blur the function v, and sometimes fail

to preserve important features. Note that this peculiar scheme of linear isotropic distribution within the anisotropic distribution is obviously against the spirit of the anisotropic distribution. So, it is clear that the isotropic distribution for function v is not an optimal choice. Thus, one issue of the distribution algorithms is how to design an anisotropic distribution for the function v in order to form a proper distribution coefficient, which can not only remove the noise from images, but also preserve the detail features well.

3.2. **Paired anisotropic distribution model.** The distribution algorithm described in Section 2 has many desirable properties. But, it still has difficulties when images are contaminated by a large noise. The main problem is that all those choices for v involve an isotropic smoothing process, which at times may cause failure in preserving important corners and junctions, and may also cause failure to resolve small features that are closely grouped together.

Inspired by the relationship proposed by You et al. [26] between energy minimization and anisotropic distribution equation, we consider choosing the function v to minimize the following energy functional,

$$E_u(v) = \int_\Omega \frac{1}{2}\phi(|\nabla u|)|\nabla u|^2 + \frac{1}{2}\varphi(|\nabla u|)|v - f|^2 dx, \tag{3.1}$$

where, f represents the magnitude of the original image gradient. The first term is referred to as the smoothing term producing a smooth varying scalar function at homogeneous region, and the second term is referred to as data term forcing the scalar function v to match f at the boundary of objects where $\varphi(|\nabla u|)$ is large. The weighting functions, $\phi(.)$ and $\varphi(.)$, are applied to the smoothing term and the data term, respectively. Since we want v to be smooth at locations far from the edges, but to conform to f near the edges, $\phi(.)$ and $\varphi(.)$ should be monotonically non-increasing and non-decreasing functions of $|\nabla u|$, respectively. Thus, it makes the distribution process behave well even for a large noisy image. These weighing functions depend on the gradient norm of the smoothed image u which is spatially and temporally varying, so they are also spatially and temporally varying. There are many ways to specify such pairs of weighting functions. Here, we use the following weighing functions for the distribution coefficient:

$$\phi(|\nabla u|) = exp\left(-\left(\frac{|\nabla u|}{K}\right)\right) \tag{3.2}$$

and

$$\varphi(|\nabla u|) = 1 - \phi(|\nabla u|). \tag{3.3}$$

The specification of K determines to some extent the degree of trade-off between the smoothness and the gradient conformity. The characteristics of the two weighting functions with respect to the image gradient ∇u are plotted in Fig. 1. From the figure, we can see that the function v will conform to the image gradient at strong edges, but it will be smooth away from the boundaries.

By obtaining the corresponding energy descent equation for (3.2), we propose to determine v by solving the nonlinear distribution equation:

$$\begin{aligned} \frac{\partial v}{\partial t} &= div(\phi(|\nabla u|)\nabla v) - \varphi(|\nabla u|)(v - f) \\ &= \nabla\phi(|\nabla u|)\nabla v + \phi(|\nabla u|)\nabla^2 v - \varphi(|\nabla u|)(v - f) \end{aligned} \tag{3.4}$$

We note that if $\nabla\phi(|\nabla u|)\nabla v = 0$, then (**??**) will reduce to the following equation:

$$\frac{\partial v}{\partial t} = \phi(|\nabla u|)\nabla^2 v - \varphi(|\nabla u|)(v - f). \tag{3.5}$$

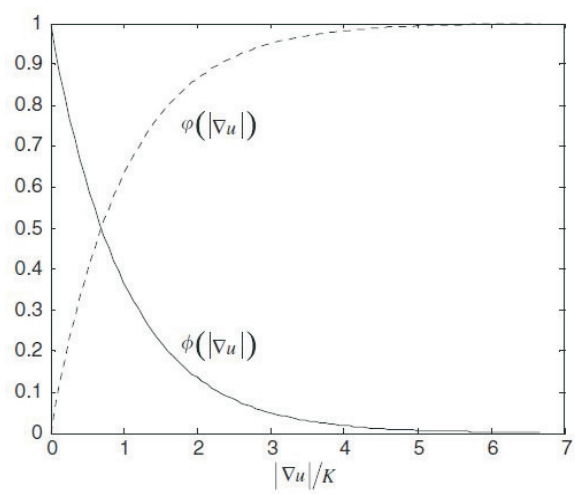

FIGURE 1. Weighing functions plotted as a function of image gradient.

However, this condition, $\phi(|\nabla u|).\nabla v = 0$, is dependent on the image data, and is satisfied within homogeneous regions, but is generally nonzero near the edges [25]. After implementing (**??**) and (**??**), we have found out that the reduced distribution coefficient has similar properties as (**??**). What is more, this reduced version is computationally more efficient. Therefore, although (**??**) does not have the aesthetically pleasing property of satisfying a minimum principle and does not lead to an exact solution of (3.2), we appreciate (**??**) if the proposed anisotropic algorithm is used.

The anisotropic distribution equation for image smoothing is as follows [22]:

$$E_v(u) = \int_\Omega \frac{1}{2} g(|v|)|\nabla u|^2 + \frac{\rho}{2}|u - I|^2 dx. \tag{3.6}$$

Function v, being the solution of anisotropic distribution of image gradient f, is introduced into (3.2) to form a regularized distribution coefficient. The solution of (3.2) can be obtained by computing the steady state of the following distribution equation:

$$\frac{\partial u}{\partial t} = div(g(|v|)|\nabla u|) - \rho(u - I). \tag{3.7}$$

Finally, our proposed model is formed by (**??**) and (**??**) together with the insulated boundary conditions and initial conditions, as shown below:

$$\begin{cases} \dfrac{\partial u}{\partial t} = div(g(|v|)|\nabla u|) - \rho(u - I) \\ \dfrac{\partial v}{\partial t} = \phi(|\nabla u|)\nabla^2 v - \varphi(|\nabla u|)(u - I) \\ \left.\dfrac{\partial u}{\partial n}\right|_{\partial\Omega} = 0 \ , \ \left.\dfrac{\partial v}{\partial n}\right|_{\partial\Omega} = 0. \end{cases} \tag{3.8}$$

The paired partial differential equations (**??**) consist of anisotropic distribution equations, which will smooth regions and diffuse the function v where the gradient is small, but will preserve them well where the gradient is large. The proposed nonlinear partial differential equations can be efficiently implemented by a concise and efficient scheme. In the next section, we will see that the proposed model obviously outweighs the others.

4. **Simulation and experimental results**

To verify the proposed paired anisotropic distribution algorithm described in the last section, we have applied this algorithm to a variety of images. In this section, two synthesis images and a real chip substrate image are chosen to demonstrate the ability of the proposed algorithm to faithfully preserve features of several structures in the presence of noise, and experimental results are presented. Furthermore, applying

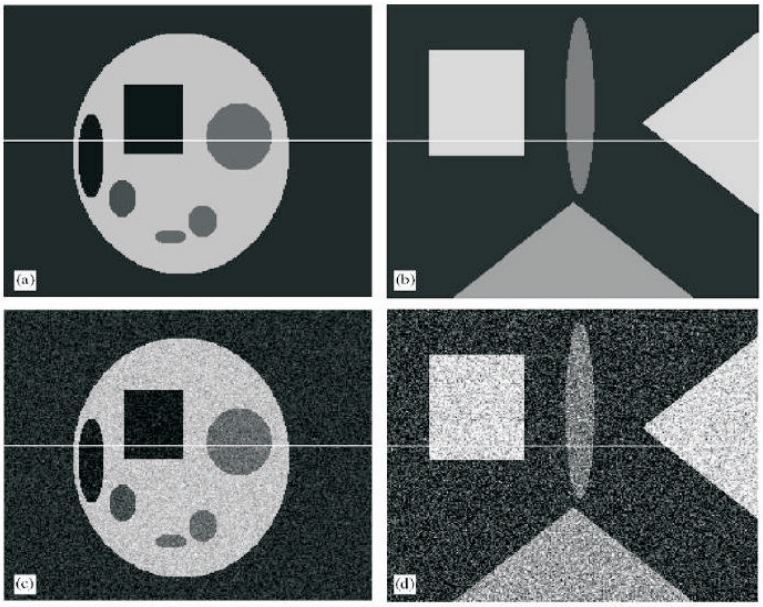

FIGURE 2. Synthetic piece-wise constant grey-scale images: (a) original image, (b) original image, (c) noisy image (Gaussian noise with 10.2 dB), and (d) noisy image (Gaussian noise with 3.2 dB).

the model in (**??**) and our proposed model in (**??**) on synthesis data, we do some comparisons of the results. During the experiments, we chose parameters in these models giving optimal results by trial and error.

To evaluate the filtering quality in the simulations, we need the notion of distance between two images. The Euclidean distance seems most suited for theoretical analysis [11], and has the ability of evaluating the difference between two images. In our experiments, the Euclidean

distance between two images is defined as follows:

$$Distance = \sum_{i=1}^{m} \sum_{j=1}^{n} [u(i,j) - I(i,j)]^2. \tag{4.1}$$

Another note concerns the simulation of the noise in these images. Degrading a discrete image I to the noisy version of I is obtained by adding pseudorandom Gaussian noise with signal to noise ratio (SNR) ε dB, where,

$$\varepsilon = 10 \log_{10} \frac{Var(Image)}{Var(Noise)}. \tag{4.2}$$

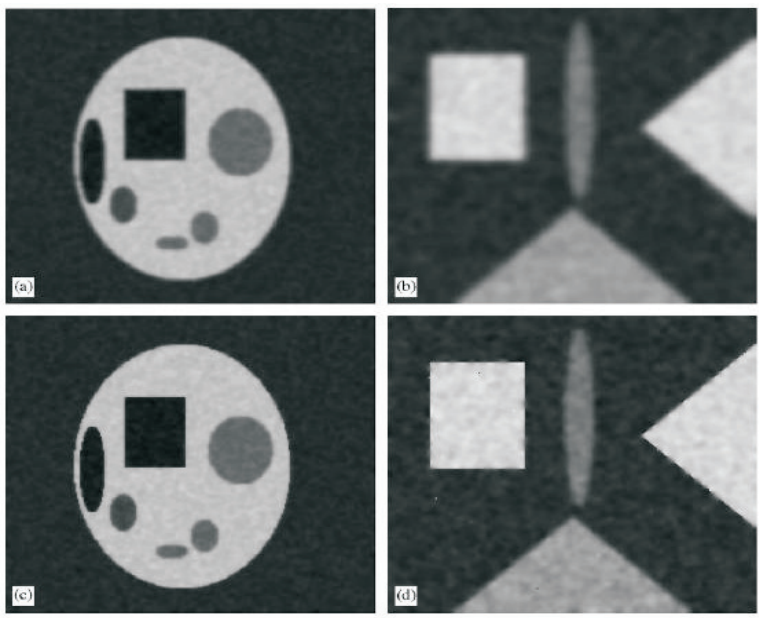

FIGURE 3. Results on synthesis data: (a), (b) smoothed images by Catte's algorithm, (c), (d) smoothed images by the proposed algorithm.

The original images only contain intensities between 0 and 255; adding the additive pseudorandom Gaussian noise makes pixel values of noisy image outside of the range. It seems that it is customary to always truncate values of the noisy pixel values outside of [0, 255] so that they are in that range. However, here we do not truncate the noisy pixel

values, so our noisy images contain intensities well outside the [0, 255] range. For instance, the noisy image in Fig. 2 contains intensities as low as -47 and as high as 312. This presents a much greater challenge to the algorithm than the truncated version.

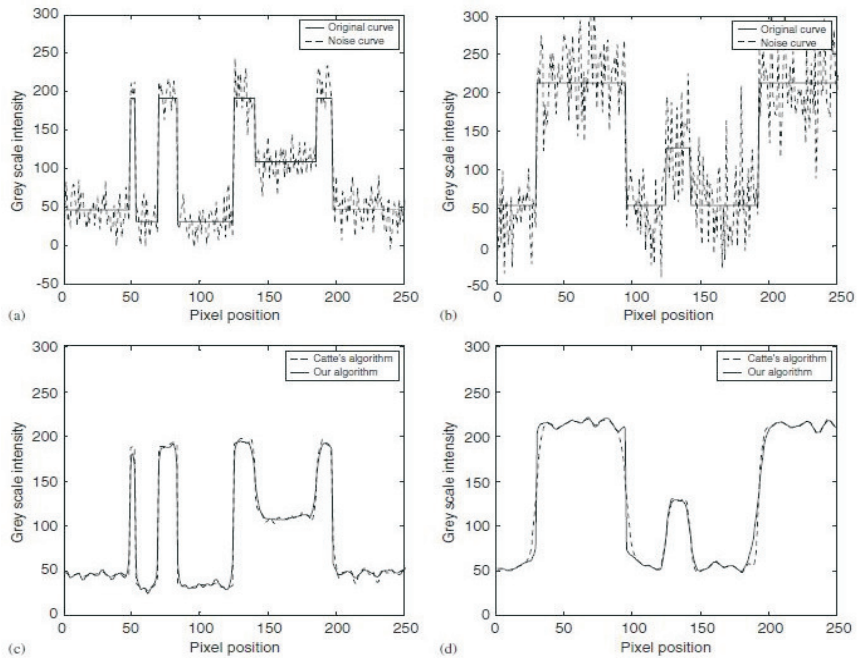

FIGURE 4. Cross-sections of images: (a), (b) cross-sections of original image and noisy image, (c), (d) cross-sections of smoothed image by the proposed algorithm and one by Catte's algorithm.

Figs. 2(a) and 2(b) show the synthesis images, which are grey-scale and piece-wise constant objects and are represented on a 256×256 square lattice. There are a lot of typical features that are used to demonstrate the ability of the proposed algorithm. For the first image, pseudo-random Gaussian noise with SNR 10.2 dB is added to the original image to obtain the noisy version shown in Fig. 2(c). The Catte's model is run with $k = 56, \delta = 0.05, \Delta t = 0.05$ for 68 iterations, and produces the smoothed image shown in Fig. 3(a), whose distancens with $k = 45, K = 36, \Delta t = 0.05$. This produces the smoothed image shown

in Fig. 3(c), whose distance is 1379.2. For the second image, pseudo-random Gaussian noise with SNR 3.2 dB is added to the original image to obtain the noisy version shown in Fig. 2(d). The Catte's model is run with $k = 68, \delta = 0.2, \Delta t = 0.05$ for 106 iterations, and produces the smoothed image shown in Fig. 3(b), whose is 1922.0. The proposed model is run for 43 iteratio distance is 3728.8.0. The proposed model is run for 74 iterations with $k = 53, K = 43, \Delta t = 0.05$. This produces the smoothed image shown in Fig. 3(d), whose distance is 2468.0. We see that our method requires less rounding of sharp corners and gives better enhancements.

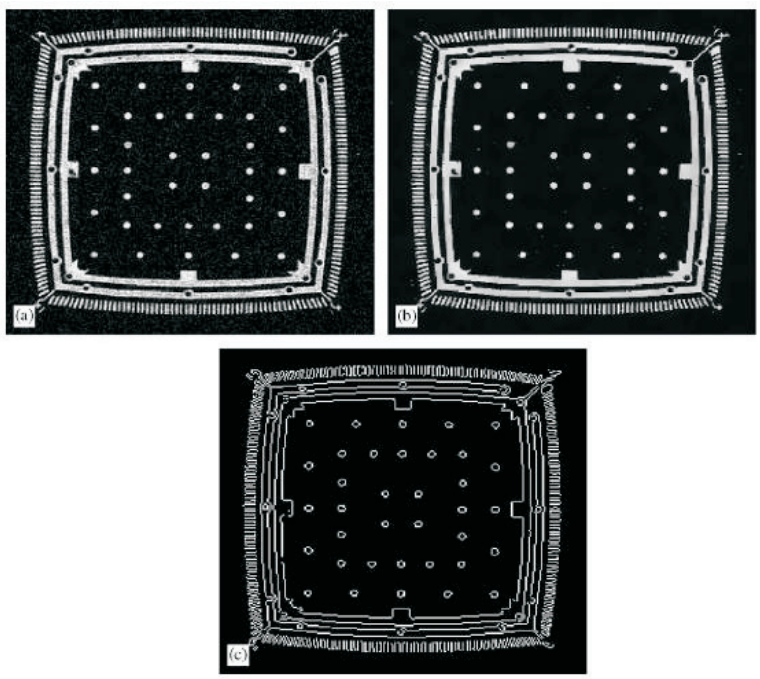

FIGURE 5. Experimental results on real chip substrate image: (a) real picture of a chip substrate, (b) smoothed substrate image by the proposed algorithm, (c) edge map of smoothed image.

In order to see the improvement of the proposed model clearly, line plots of particular rows of the true, noisy and smoothed images are presented in Fig. 4. Figs. 4(a) and 4(b) contain line plots of the 120th

row of the true and noisy images. Line plots for the same section in the smoothed images produced by two different algorithms are shown in Figs. 4(c) and 4(d), respectively. From these figures, we can see clearly that the large noise image smoothed by Catte's method is more blurred, so produces rounded edges, and the locations of edges are worse, but we do not expect these rounded edges and the false ones to appear in real applications. Nevertheless our proposed algorithm obtains good quality images and preserve the details of the features well.

Fig. 5(a) is an actual digital photograph of a chip substrate. The smoothed image and edge map in Figs. 5(b) and (c) are obtained by running the discretization of the proposed model (**??**) for eight iterations with $k = 15, K = 20, \Delta t = 0.15$. The edges or the features are very important for vision location and quality inspection.

Acknowledgment

This research was supported by the research Council of the University of Zabol.

References

[1] L. Alvarez, P. Lions, J. Morel, Image selective smoothing and edge detection by nonlinear diffusion II, *SIAM J. Numer. Anal.* **29** (3) (1992) 845-866.

[2] M. Black, G. Sapiro, D. Marimont, D. Heeger, Robust anisotropic diffusion, *IEEE Trans. Image Process.* **7** (3) (1998) 421-432.

[3] V. Caselles, J. Morel, G. Sapiro, A. Tannenbaum, Introduction to the special issue on partial differential equations and geometry-driven diffusion in image processing and analysis, *IEEE Trans. Image Process.* **7** (3) (1998) 387-397.

[4] F. Catte, P.-L. Lions, J. M. Morel, T. Coll, Image selective smoothing and edge detection by nonlinear diffusion, *SIAM J. Numer. Anal.* **29** (1) (1992) 182-193.

[5] P. Charbonnier, L. Blanc, G. Aubert, M. Barlaud, Two deterministic half-quadratic regularization algorithms for computed imaging, *IEEE International Conference on Image processing, Austin, TX*, **vol. 2**, 1994, pp. 168-172.

[6] Y. Chen, C. Barcelos, B. Mair, Smoothing and edge detection by time-varying coupled nonlinear diffusion equations, *Comput. Vision Image Understand.* **82** (2001) 85-100.

[7] I. Dolcetta, R. Ferretti, Optimal stopping time formulation of adaptive image filtering, *Appl. Math. Optim.* **43** (2001) 245-258.

[8] L. Feraud, P. Charbonnier, G. Aubert, M. Barlaud, Nonlinear image processing: modeling and fast algorithm for regularization with edge detection, *IEEE International Conference on Image process, Washington, DC,* **vol. 1**, 1995, pp. 474-477.

[9] S. Kichenssamy, The Perona-Malik paradox, *SIAM J. Appl. Math.* **57** (5) (1997) 1328-1342.

[10] J. Kim, A. Tsai, M. Cetin, A. Willsky, A curve evolutionbased variational approach to simultaneous image restoration and segmentation, *IEEE International Conference on Image process,* **vol. 1,** 2002, pp. 109-112.

[11] P. Mrazek, M. Navara, Selection of optimal stopping time for nonlinear diffusion filtering, *Int. J. Comput. Vision* **52** (2003) 189-203.

[12] P. Mrazek, Monotonicity enhancing nonlinear diffusion, *J. Visual Comm. Image Represent.* **13** (2002) 313-323.

[13] D. Mumford, J. Shah, Optimal approximation by piecewise smooth functions and associated variational problems, *Comm. Pure Appl. Math.* **42** (1989) 577-685.

[14] M. Nitzberg, T. Shiota, Nonlinear image filtering with edge and corner enhancement, *IEEE Trans. Pattern Anal. Mach. Intell.* **14** (8) (1992) 826-833.

[15] P. Perona, J. Malik, Scale-space and edge detection using anisotropic diffusion, *IEEE Trans. Pattern Anal. Mach. Intell.* **12** (7) (1990) 629-639.

[16] G. Sapiro, From active contours to anisotropic diffusion: connections between basic PDEs in image processing, *IEEE International Conference on Image process, Lausanne, Switzerland,* **vol. 1**, 1996, pp. 477-480.

[17] J. Sethian, Level Set Methods and Fast Marching Methods, *Cambridge University Press, Cambridge,* 1996.

[18] J. Shah, A common framework for curve evolution, segmentation and anisotropic diffusion, *IEEE Computer Society Conference on Computer Vision and Pattern Recognition, San Francisco, CA,* 1996, pp. 136-142.

[19] T. Tasdizen, Ross. Whitaker, P. Burchard, S. Osher, Geometric surface smoothing via anisotropic diffusion of normals, *Proc. IEEE Visual.* (2002), pp. 25-132.

[20] S. Teboul, S. Teboul, L. Blane, G. Aubert, M. Barlaud, Variational approach for edge-preserving regularization on using coupled PDEs, *IEEE Trans. Image Process.***7** (3) (1998) 387-397.

[21] B. Vemuri, L. Wang, C. Yunmei, A Coupled PDE model of nonlinear diffusion for image smoothing and segmentation, *IEEE Computer Society Conference on Computer Vision and Pattern Recognition, Santa Barbara, CA,* 1998, pp. 132-137.

[22] J. Weickert, A review of nonlinear diffusion filtering,*Scale-Space Theory in Computer Vision, Lecture Notes in Computer Science* **1252** (1997) 3-28.

[23] J. Weickert, Applications of nonlinear diffusion in image processing and computer vision, *Acta Math. Univ. Comenianae, vol. LXX* **(1)** (2000) 33-50.

[24] A. Witkin, Scale-space filtering, in:*Proceeding of the Eighth International Joint Conference on Artificial Intelligence, William Kaufmann Inc., Karlsruhe, Germany,* 1983, pp. 1019-1021

[25] C. Xu, J. Prince, Generalized gradient vector flow extern forces for active contours, *Signal Process.* **71** (1998) 131-139.

[26] Y. You, W. Xu, A. Tannenbaum, M. Kaveh, Behavioral analysis of anisotropic diffusion in image processing, *IEEE Trans. Image Process.* **5** (11) (1996) 1539 - 1553.

A. Madankan
Department of Computer Science, University of Zabol, Zabol, Iran
Email: amadankan@gmail.com